and synaptotagmin 1. All blots were hybridized with a GAPDH probe to control for RNA loading. ^{32}P signals were quantified by PhosphorImager detection and are expressed as ratio to GAPDH.

8. A rat brain cDNA library in the yeast-two hybrid prey vector pVP16 [A. B. Vojtek, S. M. Hollenberg, J. A. Cooper, *Cell* **74**, 205 (1993)] was screened as described [S. Fields and O. Song, *Nature* **340**, 245 (1994)] (*14*) with the bait vector pBTM116-NL2-1 (*8*). Of 16 prey clones isolated, pPrey500 encodes residues 1 to 287, and pPrey514 encodes residues 308 to 425 of PSD-95 (*1*). β-Galactosidase assays were corrected for protein concentration [M. D. Rose, F. Winston, P. Hieter, *Methods in Yeast Genetics* (Cold Spring Harbor Laboratory Press, Cold Spring Harbor, NY, 1990); Y. Hata and T. C. Südhof, *J. Biol. Chem.* **270**, 13022 (1995)].
9. The full-length sequence of rat PSD-95 (residues 1 to 724), its NH_2-terminus (residues 1 to 431), and its COOH-terminus (residues 430 to 724) were cloned by PCR with oligonucleotides 1176 (GCGCTCGAGGTACCATGGACTGTCTCTGTATAGTGAC), 1177 (CGCGTCGACTAGAAGCCCCTCTTGGGGTT), 1178 (CGCCTCGAGGAATCAGAGTCTCTCTCGGGC), and 1198 (GCGAATTCTCCATGGGCTTCTACATTAGGGCC). To identify additional members of the PSD-95 family, we used a degenerate PCR strategy. Products from PCRs with redundant oligonucleotide primers complementary to conserved sequences (T73 = TICCI-[C,T]A[C,T]ACIACI[C,A]GICC;T75=AC[G,A]TCIA-[G,A]IAT[G,A]CA[G,A]TG; T76 = GGIGA[C,T]ATI-[C,T]TICA[C,T]GT; I = inosine; brackets = redundant positions) were subcloned and sequenced. We used two products (A290 and A309) containing unusual sequences related to PSD-95 as probes to isolate full-length clones pDLG54 and pDLG70 (GenBank accession numbers U53367 and U53368). The same two isoforms have been independently reported as PSD-93/chapsyn and SAP102 (*1*). pDLG54 is identical with SAP102 except for the absence of the sequence VTSNTSDSESSSKG (residues 627 to 630) (*17*), which suggests that pDLG54 represents a splice variant of SAP102. pDLG70 corresponds to PSD-93/chapsyn with several amino acid differences that may be due to alternative splicing or sequencing variations. The neuroligin bait vectors used encode the following residues of the rat proteins (*4*): pBTM116-NL1-1, 718–843; pBTM116-NL1-2, 718–840; pBTM116-NL1-5, 718–828; pBTM116-NL1-6, 828–843; pBTM116-NL1-10, 796–843; pBTM116-NL2-1, 699–836; pBTM116-NL2-2, 699–786; pBTM116-NL2-3, 786–836; pBTM116-NL3, 730–848. The NMDA2 receptor bait plasmids encode residues 1455–1464 (pBTM116NMDAR2A) and 1473–1482 (pBTM116NMDAR2B) of the rat NMDA-2A and -2B receptors. pBTM116Shaker encodes residues 645–654 of the rabbit Kv1.4 K^+ channel isoform. The different prey vectors are from rat except for ZO-1 (mouse) and *dlg-A* (*Drosophila*) and encode the following residues: PSD-95, pVP16PSD-95-2 = 1–431; pVP16SAP90-5 = 69–150; pVP16SAP90-6 = 160–245. SAP102, pVP16SAP102-1 = 1–519. PSD-93, pVP16PSD-93-1 = 1–539. ZO1, pVP16ZO1-1 = 1–500. *dlg-A*, pVP16dlg-1 = 1–598. Nitric oxide synthase, pVP16NOS = 1–101.
10. D. A. Doyle *et al.*, *Cell* **85**, 1067 (1996).
11. Synthetic peptides were purified on a Kromasil 100 C_{18} reversed-phase column (sequences: NMDAR2A, SNRRVYKKMPSIESDV; NL1-1, LPHPHPHPHSHSTTRV; NL1-2, LPHPHPHPHSHST; control, KFIEAGQYNSHLYGTSV). NMDAR2A and NL1-1 correspond to the COOH-terminus of NMDA2A and neuroligin 1, respectively. NL1-2 is identical with NL1-1 except it lacks the last three amino acids. The control peptide is composed of residues 597 to 613 from PSD-95/SAP90. Peptides were immobilized on a CM5 research grade sensor chip with the amine coupling kit (Pharmacia), equilibrated with 50 mM Hepes-NaOH (pH 8.0) containing 100 mM NaCl, and superfused with GST fusion proteins at different concentrations (flow rate, 20 μl/min). Binding activities (in resonance units) were measured as the difference between the baseline value determined 10 s before sample injection and the measurements taken at the indicated time points. All experiments were performed at 25°C. Data were analyzed with the BIA Evaluation program 2.1 (Pharmacia) [U. Joehnsson *et al.*, *BioTechniques* **11**, 520 (1991)].
12. IgG fusion proteins of the extracellular domains of neurexin 1β with and without an insert in splice site 4 and control IgG fusion protein were purified from transfected COS cells (*4*). Twelve rat brains were homogenized in 48 ml of 20 mM Hepes-NaOH (pH 8.0), 1% (w/v) NP-40, 0.2 M NaCl, 2 mM EGTA, and phenylmethylsulfonyl fluoride (0.1 g/liter) in a glass Teflon homogenizer and centrifuged (100,000*g* for 60 min at 4°C). The supernatant (60 ml) was adjected to 3.5 mM $CaCl_2$. Supernatant (20 ml) (0.2 to 0.3 g of protein) was incubated overnight at 4°C with recombinant IgG fusion proteins immobilized on protein A-Sepharose. Beads were washed repeatedly by centrifugation in 20 mM Hepes-NaOH (pH 8.0), 2.5 mM $CaCl_2$, 0.2 M NaCl, and 0.5% NP-40 and eluted sequentially with 0.3 ml of the wash buffer containing 0.5 M NaCl and with 0.5 ml of 20 mM Hepes-NaOH (pH 8.0), 0.1 M NaCl, 10 mM EGTA, and 0.5% NP-40. Fractions were analyzed by SDS–polyacrylamide gel electrophoresis and by immunoblotting with antibodies to PSD-95 (polyclonal antiserum L667 and two independent monoclonal antibodies) and to neuroligin 1 (polyclonal antiserum L067). To exclude the possibility that PSD-95 directly interacts with neurexin 1β, extracts from COS cells transfected with full-length PSD-95 were affinity chromatographed on immobilized neurexin 1β in the absence and presence of recombinant neuroligin.
13. HEK293 cells were transfected with pCMVPSD95-1 encoding full-length rat PSD-95 either alone or together with pCMVNL18, pCMVNR2A, or pCMVNR1 encoding full-length neuroligin 1, NMDA2A, or NMDA1, respectively. Cells were stained with a mouse monoclonal antibody to PSD-95 and rabbit polyclonal antibodies to neuroligin 1 (L067) or the two NMDA receptors (from Chemicon). Images were obtained on a Bio-Rad MRC1024 confocal microscope.
14. Y. Hata, S. Butz, T. C. Südhof, *J. Neurosci.* **16**, 2488 (1996).
15. A. B. Russell and S. S. Carlson, *ibid.* **17**, 4734 (1997).
16. N. Uchida, Y. Honjo, K. R. Johnson, M. J. Wheelock, M. Takeichi, *J. Cell Biol.* **135**, 767.
17. Abbreviations for amino acids are as follows: A, Ala; C, Cys; D, Asp; E, Glu; F, Phe; G, Gly; H, His; I, Ile; K, Lys; L, Leu; M, Met; N, Asn; P, Pro; Q, Gln; R, Arg; S, Ser; T, Thr; V, Val; W, Trp; Y, Tyr.
18. We thank A. Roth, E. Borowicz, and I. Leznicki for excellent technical assistance; M. B. Kennedy (CalTech) for monoclonal antibodies to PSD-95; S. Nakanishi (Kyoto) for NMDA receptor cDNA clones; and M. Missler, M. S. Brown, and J. L. Goldstein for advice. Partially supported by grants from the NIH (RO1-MH52804), the Perot Family Foundation, and the ERATO (Japan Science and Technology Co.). Y.H. was supported by a postdoctoral fellowship from the HFSP, and T.W.R. from the DFG.

10 March 1997; accepted 14 July 1997

Postsynaptic Glutamate Transport at the Climbing Fiber–Purkinje Cell Synapse

Thomas S. Otis,* Michael P. Kavanaugh, Craig E. Jahr

The role of postsynaptic, neuronal glutamate transporters in terminating signals at central excitatory synapses is not known. Stimulation of a climbing fiber input to cerebellar Purkinje cells was shown to generate an anionic current mediated by glutamate transporters. The kinetics of transporter currents were resolved by pulses of glutamate to outside-out membrane patches from Purkinje cells. Comparison of synaptic transporter currents to transporter currents expressed in *Xenopus* oocytes suggests that postsynaptic uptake at the climbing fiber synapse removes at least 22 percent of released glutamate. These neuronal transporter currents arise from synchronous activation of transporters that greatly outnumber activated AMPA receptors.

The glutamate transporters EAAT3 and EAAT4 are expressed at high levels in cerebellar Purkinje cells (PCs) (*1*). Transporters on PCs exhibit substrate-induced anion currents (*2*) similar to those associated with other native (*3*, *4*) and cloned glutamate transporters (*5*–*7*). Because the conductance associated with the glutamate transporter has a high permeability to NO_3^- and SCN^- (*4*, *6*), they were used as the major intracellular anions in PC recordings. Extracellular stimulation in the granule cell layer of cerebellar slices elicited all-or-none excitatory postsynaptic currents (EPSCs), suggesting activation by single climbing fiber (CF) afferents (Fig. 1A) (*8*). These currents were mediated in part by AMPA (α-amino-3-hydroxy-5-methyl-4-isoxazolepropionic acid) receptors, because 10 to 25 μM NBQX blocked more than 95% of the current (Fig. 1A) and addition of the specific AMPA receptor antagonist GYKI 52466 (15 to 25 μM, $n = 3$) or the *N*-methyl-D-aspartate (NMDA) receptor antagonist (±)-3-(2-carboxy piperazin-4-yl)-propyl-1-phosphonic acid (CPP) (2.5 μM) caused no further inhibition. After blockade of AMPA and NMDA receptors, stimulation still activated inward currents with NO_3^- (Fig. 1B) ($n = 25$) or SCN^- ($n = 6$) but not with Cl^-- (Fig. 1B, inset) ($n = 3$) or gluconate-based ($n = 3$) pipette solutions.

Vollum Institute, L-474, Oregon Health Sciences University, 3181 Southwest Sam Jackson Park Road, Portland, OR 97201, USA.

*To whom correspondence should be addressed.

With Cl^- in the extracellular solution, these responses displayed current-voltage (*I-V*) relations with the reversal potential >+50 (Fig. 1B) indicating a high permeability to NO_3^- and SCN^-. AMPA receptor EPSCs in the same recordings reversed at −6 ± 2 mV (n = 6). Both the AMPA receptor EPSCs and the synaptic, anionic currents were all-or-none with identical stimulation thresholds, indicating that they resulted from activation of the same CF (Fig. 1C). Anionic currents were antagonized by glutamate transporter antagonists L-*trans*-2,4-pyrrolidine dicarboxcylic acid (PDC, 300 μM), D,L-*threo*-β-hydroxyaspartic acid (THA, 300 μM), and the EAAT4-preferring substrate L-α-amino-adipate (L-AA, 500 μM), but were unaffected by the EAAT2-specific antagonist dihydrokainic acid (DHK, 300 μM) (Fig. 1D) (*5*, *9*, *10*). As expected from their activities as transported substrates, application of PDC, THA, and L-AA activated large inward currents (Fig. 1D). Consistent with its immunolocalization in PCs (*1*), these results indicate that CF stimulation activates a postsynaptic glutamate transporter current mediated at least in part by the glutamate transporter EAAT4.

The density and localization of functional glutamate transporters in the synaptic cleft is not known, but will affect their ability to regulate the glutamate concentration transient in the cleft and could prevent glutamate from "spilling over" to neighboring synapses. If transporters are distant from release sites, then their initial activation may be delayed and the rise time of the PC synaptic transporter current (STC) may be slowed by diffusion. The initial points of rise from the baseline noise of CF EPSCs and STCs were not different (0.1 ± 0.2 ms, n = 10, $P > 0.3$), suggesting that some transporters are located very near release sites. However, the STC rises more slowly than the EPSC (Fig. 2A) (20 to 80% rise time: 2.63 ± 0.31 ms versus 0.37 ± 0.03 ms) and decays with two exponential components, both slower than the two components of the EPSC decay (τ_{FAST} = 28 ± 4.8 ms versus 3.8 ± 0.23 ms; τ_{SLOW} = 94 ± 16 ms versus 17 ± 0.9 ms: fraction of fast component = 76 ± 5% versus 70 ± 7% for STCs and EPSCs, respectively; n = 9).

To determine whether the rising and decaying kinetics of the STC were slower than those of the EPSC because of diffusional delays or slower intrinsic kinetic properties of the transporter conductance, we measured the kinetics of the transporter current activated in outside-out patches by rapid applications of L-glutamate in the presence of AMPA and NMDA receptor antagonists (*11*). Brief pulses (0.8 to 2 ms) of 2 mM L-glutamate gave transient responses that were blocked by THA (Fig. 2B) (300 μM, n = 7) and antagonized by PDC (300 μM: 9 ± 1% remaining, n = 3). Longer applications (>2 ms) resulted in the appearance of a sustained component (Fig. 2B). In addition, six of six patches responded to pulses of 10 mM D-aspartate, an amino acid that elicits transporter current (*5*, *6*, *10*). Rise times (20 to 80%) of the transient current were 0.75 ± 0.08 ms (n = 6) in response to brief pulses of 2 mM glutamate. The decay of patch responses elicited by 1-ms glutamate pulses (2 mM) were well fitted by a single exponential time course (τ = 7.8 ± 0.8 ms; n = 6). The slower rise and decay of the synaptic responses to glutamate may be the result of asynchronous release, dendritic filtering, diffusion to some distantly located transporters, and a slow phase of clearance at the synapse (*12*–*14*) that cannot be reproduced in the patch experiments. Together these data indicate that postsynaptic transporters are exposed to a rapid transient of glutamate after release by CF terminals.

Transmitter removal at many synapses in the central nervous system may require transporters on postsynaptic neurons as well as on surrounding glial cells (*1*). STCs can be used to estimate the number of glutamate molecules transported into the PC in response to CF activation.

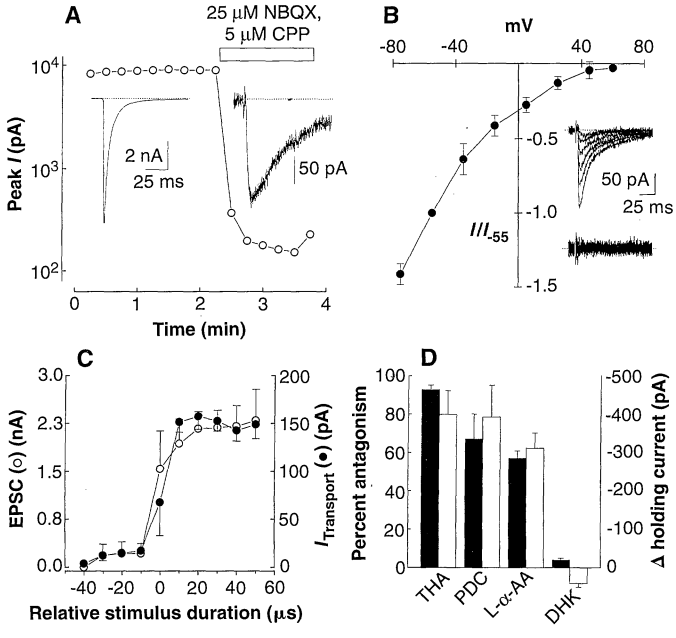

Fig. 1. Climbing fiber stimulation elicits anion currents associated with glutamate transport. (**A**) With 130 mM NO_3^- in the pipette and 100 μM picrotoxin in the bath, CF EPSCs are strongly diminished by 25 μM NBQX and 5 μM CPP. (**Insets**) Means of three successive responses before and after blockade of AMPA and NMDA receptors. V_m = −25 mV. (**B**) *I-V* relation for the response in NBQX and CPP (n = 10 PCs). (**Insets**) Responses at different V_m's (−80 to +20 mV, ΔV = 20 mV) recorded from a PC filled with NO_3^- (top) and from a different PC filled with Cl^- (bottom). (**C**) The threshold for the CF EPSC was determined (mean: 50 μs) by changing stimulus duration in 10-μs increments; stimulus intensity is expressed as the change relative to the threshold intensity. At each intensity the average peak response was determined for two to four trials; the mean of failures and successes accounts for the intermediate amplitude level at 0 μs. After blocking ionotropic receptors, stimuli were delivered over the same range of intensities. Mean peak amplitudes before (○) and after (●) NBQX/CPP are plotted versus relative stimulus intensity for three PCs. (**D**) Transported antagonists (THA, n = 8; PDC, n = 6; and L-α-AA, n = 7) that inhibit (filled bars) the NBQX-insensitive response also elicit inward currents (open bars), whereas a glial-specific antagonist, DHK (n = 2), is without effect.

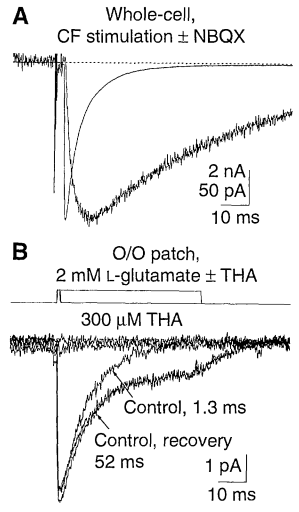

Fig. 2. Kinetics of transporter currents evoked by synaptic release and by glutamate pulses to outside-out patches. (**A**) Superimposition of a normalized CF EPSC (smooth trace) and an STC (noisy trace). V_m = −36 mV. (**B**) Outside-out patch responses (below) to pulses of 2 mM L-glutamate (1.3- and 52-ms duration) before, during 300 μM THA application, and after recovery of the response (52-ms pulse only). The open-tip currents (above) illustrate the time course of solution exchange. V_m = −80 mV.

Charge movement during transport results from the sum of coupled ionic movements (1 K^+ countertransported, 3 Na^+ and 1 H^+ cotransported with 1 glutamate) and the flux of anions that are not stoichiometrically coupled to substrate movement (*5*, *6*, *15*). If the total amount of charge flux per cycle is known, the number of glutamate molecules transported into a PC can be estimated. Simultaneous measurements of radiolabeled glutamate and charge flux were made from oocytes expressing either EAAT4 or EAAT3 and containing 30 to 35 mM intracellular NO_3^- (Fig. 3) (*16*). Specific uptake in EAAT4-expressing oocytes was 35 ± 7 fmol/s and the ratio of charge to glutamate flux was 33 ± 6 elementary charges (e^-) per glutamate molecule (n = 7); for EAAT3-expressing cells, the values were 547 ± 120 fmol/s and 2.6 ± 0.1 e^- per glutamate molecule (n = 8). These results are consistent with a higher expression level or turnover rate of EAAT3 relative to EAAT4 (or both), and the report that most of the EAAT4 current is due to anion flux (*5*). CF elicited EPSCs (Fig. 4A), and STCs (Fig. 4B) were recorded with gradients of permeant anions identical to those used for the oocyte flux measurements (*17*). The normalized *I-V* curve for STCs recorded with this pipette solution (Fig. 3, filled circles; n = 4 to 8) matches the *I-V* curves from oocytes expressing EAAT4 (Fig. 3A, open circles; n = 8) and EAAT3 (Fig. 3B, open circles, n = 7). STCs were integrated to yield a mean charge of 1.5 ± 0.2 pC (n = 10). The charge/flux measurements obtained for EAAT3 and EAAT4 permit upper and lower estimates, respectively, of the number of glutamate molecules transported during the STC. If the STC is mediated solely by EAAT4, then $2.8 \times 10^5 \pm 0.3 \times 10^5$ glutamate molecules are transported. If EAAT3 is the sole transporter type, then $3.7 \times 10^6 \pm 0.4 \times 10^6$ glutamates are transported (n = 10). Although these experiments cannot determine the relative contributions of any transporter subtype precisely, the estimate of charge transfer/glutamate flux for EAAT4 places a lower limit on the number of glutamate molecules transported into the PC during CF synaptic transmission.

The number of glutamate molecules released was estimated by measuring the quantal content of the CF EPSC corresponding to each STC. Charge movement associated with a quantum of transmitter was measured by recording asynchronous quantal events (aEPSCs) after CF EPSCs evoked in a solution containing 0 $CaCl_2$, 0.5 mM $SrCl_2$, 3.3 mM $MgCl_2$ (n = 3 PCs) (Fig. 4, C and D) (*18*). Quantal content of CF EPSCs was estimated to be 385 ± 57 (n = 10). Assuming that 4000 molecules of transmitter are contained in each vesicle (*19*), these data predict that postsynaptic transport by EAAT4 would be expected to remove 880 molecules per active release site or 22 ± 4% (n = 10) of glutamate released at the CF synapse.

Previous studies have shown that inhibition of transporters prolongs the decay of CF EPSCs (*14*) and EPSCs in other preparations (*12*, *20*). We have found that transporters located on Purkinje neurons remove a substantial fraction of the glutamate released by CF contacts. Other pathways for glutamate removal include diffusion, transport into Bergmann glia (*21*), and possibly CF terminals. The transport-associated currents observed in response to CF stimulation and in patches have surprisingly rapid kinetics, given the slow turnover rates of glutamate transporters (*22*, *23*). The fast rise of these currents may result from localization of transporters near release sites allowing rapid, nearly synchronous binding of glutamate to the large fraction of the transporter population that at negative membrane potentials is already bound by Na^+ (*23*). Similar synchronous activation of transporters has been reported at serotonergic synapses in the leech (*24*). The rapid activation of these currents also indicates that the anion conductance associated with glutamate transporters opens soon after glutamate binding.

Assuming the pulse of glutamate in the cleft is too short to result in multiple transport cycles, at least 880 EAAT4 transporters are required to be bound per exocytotic event. Because EAAT3, which has a much lower anion flux per transport cycle than EAAT4, is also expressed in PCs (*1*), the number of transporters activated by each quantal event may be even higher. Given AMPA receptor channel conductances (*25*) and mEPSC amplitudes from this study, ~50 AMPA receptors are activated by a vesicle of transmitter. Thus, transporters activated by the contents of a single vesicle outnumber activated receptors by a ratio of greater than 15 to 1. Such a large population of transporters located near release sites will

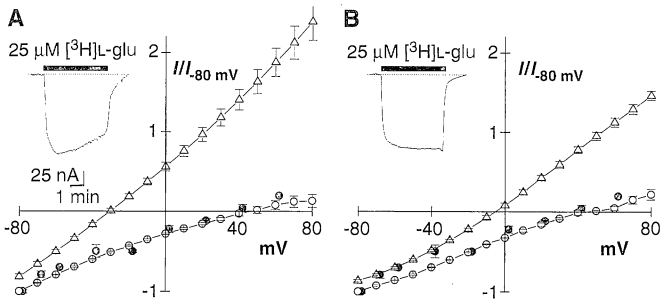

Fig. 3. Determination of the number of charges per glutamate molecule transported by EAAT4 or EAAT3. (**A**) Normalized *I-V* plots for EAAT4-injected oocytes incubated in 96 mM NO_3^-. (△) *I-V* relation in the high-$[NO_3^-]_{out}$ incubation solution. Radiolabeled flux measurements were made with a solution containing permeant anion concentrations identical to those used in the brain slice experiments, and the *I-V* curve for EAAT4-expressing oocytes in this solution (○, n = 8) matches the *I-V* curve for the peak of the STC (●, n = 4 to 8). (**Inset**) Membrane current recorded from an EAAT4-injected *Xenopus* oocyte voltage-clamped at −55 mV in response to 25 μM [^{3}H]L-glutamate. (**B**) *I-V* curves for EAAT3-expressing oocytes and the peak STC as in (A) (n = 7). (**Inset**) Membrane current in an EAAT3-injected *Xenopus* oocyte in response to 25 μM [^{3}H]L-glutamate.

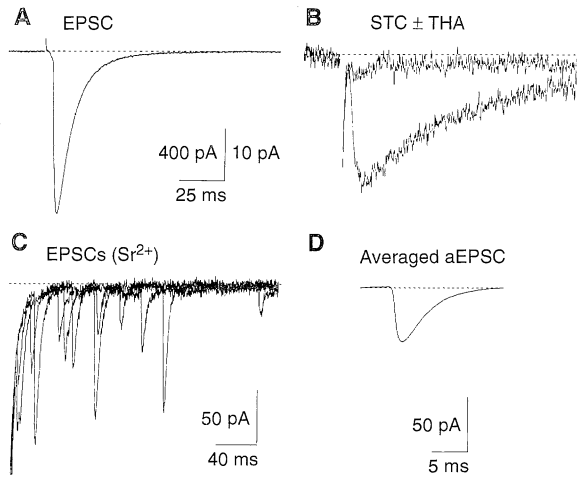

Fig. 4. Estimation of CF quantal content and uptake by the PC. (**A**) CF EPSC recorded at −25 mV with 35 mM NO_3^- in the recording pipette. (**B**). The STC recorded in the same cell at −60 mV in 25 μM NBQX, 25 μM GYKI 52466, and 2.5 μM CPP ± 300 μM THA. (**C**) Three traces showing asynchronous release of unitary EPSCs (aEPSCs) in response to CF stimulation in Sr^{2+}. (**D**) Average of 188 aEPSCs collected from 100 stimuli delivered to the CF synapse in (C). Integration yielded 242 pC. V_m = −85 mV.

both speed the clearance and help restrict the spread of glutamate, first by binding and then transporting the transmitter (26).

REFERENCES AND NOTES

1. J. D. Rothstein *et al.*, *Neuron* **13**, 713 (1994); K. Yamada *et al.*, *Neuroreport* **7**, 2013 (1996); Y. Kanai, P. G. Bhide, M. DiFiglia, M. A. Hediger, *ibid.* **6**, 2357 (1995).
2. M. Takahshi, M. Sarantis, D. Attwell, *J. Physiol.* **497**, 523 (1996); Y. Kataoka and H. Ohmori, *J. Neurophysiol.* **76**, 1870 (1996).
3. G. B. Grant and J. E. Dowling, *J. Neurosci.* **15**, 3852 (1995); S. A. Picaud, H. P. Larsson, G. B. Grant, H. Lecar, F. S. Werblin, *J. Neurophysiol.* **74**, 1760 (1995); B. Billups, D. Rossi, D. Attwell, *J. Neurosci.* **16**, 6722 (1996).
4. S. Eliasof and C. E. Jahr, *Proc. Natl. Acad. Sci. U.S.A.* **93**, 4153 (1996).
5. W. A. Fairman, R. J. Vandenberg, J. L. Arriza, M. P. Kavanaugh, S. G. Amara, *Nature* **375**, 599 (1995).
6. J. I. Wadiche, S. G. Amara, M. P. Kavanaugh, *Neuron* **15**, 721 (1995).
7. J. L. Arriza, S. Eliasof, M. P. Kavanaugh, S. G. Amara, *Proc. Natl. Acad. Sci. U.S.A.* **94**, 4155 (1997).
8. A. Konnerth, I. Llano, C. M. Armstrong, *ibid.* **87**, 2262 (1990); D. J. Perkel, S. Hestrin, P. Sah, R. A. Nicoll, *Proc. R. Soc. London Ser. B.* **241**, 116 (1990). Whole-cell recordings were made with infrared differential interference contrast optics at 22° to 24°C from PCs in 300-μM-thick cerebellar slices prepared from 12- to 20-day-old rats. Pipettes had resistances of 0.9 to 1.2 megohm; at the end of 34/49 recordings, R_{series} (4.8 ± 0.3 megohm; range: 2.5 to 10.9 megohm, n = 34) was determined by measuring instantaneous current in response to 5-mV steps with only the pipette capacitance canceled. R_{series} was compensated >80%. The extracellular solution contained 119 mM NaCl, 2.5 mM KCl, 2.5 mM $CaCl_2$, 1.3 mM $MgCl_2$, 1 mM NaH_2PO_4, 26.2 mM $NaHCO_3$, 11 mM glucose, and 0.1 mM picrotoxin saturated with 95% O_2–5% CO_2. Pipette solutions contained 130 mM (K^+ or Cs^+) A^-, 20 mM Hepes, 10 mM KCl or tetraethylammonium (TEA) chloride, 10 mM EGTA, and 1 mM $MgCl_2$, titrated to pH 7.3 with either CsOH or KOH; A^- denotes that NO_3^-, SCN^-, gluconate$^-$ or Cl^-, and KCl or TEA chloride was included in the K^+- or Cs^+-based solutions, respectively. Stimuli (10 to 100 V, 10 to 100 μs, 0.067 to 0.1 Hz) were delivered by means of a patch pipette filled with bath solution. Signals were filtered at 1 or 2 kHz (EPSCs) and digitized at 5 to 10 kHz. Membrane potential values have been corrected for junction potentials. Reported values are the mean ± SEM.
9. J. Ferkany and J. T. Coyle, *Neurosci. Res.* **16**, 491 (1986).
10. J. L. Arriza *et al.*, *J. Neurosci.* **14**, 5559 (1994).
11. Rapid agonist applications were made as described (*26*). Recording pipettes contained either KSCN- or $CsNO_3$- based solutions (*8*), and extracellular solution consisted of 135 mM NaCl, 5.4 mM KCl, 5 mM Hepes, 1.8 mM $CaCl_2$, 1.3 mM $MgCl_2$, 100 μM picrotoxin, 25 μM NBQX, 25 μM GYKI 52466, and 2.5 μM ±CPP (pH 7.4).
12. T. S. Otis, Y. C. Wu, L. O. Trussell, *J. Neurosci.* **16**, 1634 (1996).
13. J. D. Clements, *Trends Neurosci.* **19**, 163 (1996).
14. B. Barbour, B. U. Keller, I. Llano, A. Marty, *Neuron* **12**, 1331 (1994); M. Takahashi, Y. Kovalchuk, D. Attwell, *J. Neurosci.* **15**, 5693 (1995).
15. N. Zerangue and M. P. Kavanaugh, *Nature* **383**, 634 (1996).
16. Treatment of *Xenopus* oocytes was as described (*5*). Oocytes were injected with either human EAAT3 or EAAT4 mRNA and incubated 2 to 4 days in Ringer solution. Ten to 18 hours before recording, intracellular Cl^- was dialyzed by switching to Cl^--free Ringer solution containing 98 mM $NaNO_3$, 2 mM KNO_3, 1.8 mM Ca $gluconate_2$, 1 mM Mg $gluconate_2$, 5 mM Hepes (pH 7.5). For EAAT4, E_{rev} in this solution was −30 ± 2 mV (Fig. 3A, open triangles; n = 8). Neglecting the stoichiometrically coupled ionic current, which under these conditions is negligible for EAAT4 (*5*), the Nernst equation indicates that NO_3 achieved a concentration of 31 mM in EAAT4-injected oocytes. [^{3}H]L-glutamate uptake was measured in oocytes voltage-clamped at −55 mV (*5*) in a modified solution containing identical concentrations of permeant anions as in the slice solution [119 mM NaCl, 2.5 mM KCl, 2.5 mM $CaCl_2$, 1.3 mM $MgCl_2$, and 5 mM Hepes (pH 7.5)].
17. CF EPSCs (membrane potential V_m = −28 to −16 mV, mean V_m = −23 mV) and STCs (V_m = −63 to −52 mV, mean V_m = −58 mV) were recorded from 10 PCs with a pipette solution containing 95 mM Cs gluconate, 35 mM $CsNO_3$, 20 mM Hepes, 10 mM EGTA, and 1 mM $MgCl_2$ (n = 9). Mean EPSCs or STCs were integrated over 200 ms. Glutamate flux was estimated as the time integral of the STC divided by the mean charge/flux value for either EAAT3 or EAAT4 (*16*). These calculations assume the same proportion of anion current to glutamate flux throughout the STC as was measured at steady state in the oocyte experiments.
18. Integration of an average of aEPSCs recorded at −70 to −80 mV yielded charge, Q_{aEPSC}, which was scaled (assuming $aEPSC_{rev}$ = 0 mV and a linear relation between Q and V_m) to the appropriate V_m for the CF EPSC (mean V_m = −28 mV) in each of the 10 cells (*17*). Quantal content was then estimated as Q_{EPSC}/Q_{aEPSC} (range: 270 to 746, n = 10).
19. N. Riveros, J. Fiedler, N. Lagos, C. Munoz, F. Orrego, *Brain Res.* **386**, 405 (1986); D. Bruns and R. Jahn, *Nature* **377**, 62 (1995).
20. S. Mennerick and C. F. Zorumski, *Nature* **368**, 59 (1994).
21. T. Muller and H. Kettenman, *Int. Rev. Neurobiol.* **38**, 341 (1995).
22. N. C. Danbolt, G. Pines, B. I. Kanner, *Biochemistry* **29**, 6734 (1990); but see also E. A. Schwartz and M. Tachibana, *J. Physiol.* **426**, 43 (1990).
23. J. I. Wadiche, J. L. Arriza, S. G. Amara, M. P. Kavanaugh, *Neuron* **14**, 1019 (1995).
24. D. Bruns, F. Engbert, H. D. Lux, *ibid.* **10**, 559 (1993).
25. C.-M. Tang, M. Dichter, M. Morad, *Science* **243**, 1474 (1989); D. J. A. Wyllie, S. F. Traynelis, S. G. Cull-Candy, *J. Physiol.* **463**, 193 (1993); S. F. Traynelis, R. A. Silver, S. G. Cull-Candy, *Neuron* **11**, 279 (1993).
26. G. Tong and C. E. Jahr, *Neuron* **13**, 1195 (1994); J. S. Diamond and C. E. Jahr, *J. Neurosci.* **17**, 4672 (1997).

27. We thank D. Bergles, J. Diamond, J. Dzubay, S. Eliasof, M. Jones, and J. Wadiche for helpful suggestions and comments on the manuscript; L. Klamo, S. Eliasof, J. Wadiche, and T. Zable for assistance with the oocyte experiments; and J. Diamond for the mEPSC analysis program. Supported by NS21419 (C.E.J.) and NS33270 (M.P.K.).

30 May 1997; accepted 23 July 1997

Dynamic Molecular Combing: Stretching the Whole Human Genome for High-Resolution Studies

Xavier Michalet,* Rosemary Ekong,* Françoise Fougerousse, Sophie Rousseaux,† Catherine Schurra, Nick Hornigold, Marjon van Slegtenhorst, Jonathan Wolfe, Sue Povey, Jacques S. Beckmann, Aaron Bensimon‡

DNA in amounts representative of hundreds of eukaryotic genomes was extended on silanized surfaces by dynamic molecular combing. The precise measurement of hybridized DNA probes was achieved directly without requiring normalization. This approach was validated with the high-resolution mapping of cosmid contigs on a yeast artificial chromosome (YAC) within yeast genomic DNA. It was extended to human genomic DNA for precise measurements ranging from 7 to 150 kilobases, of gaps within a contig, and of microdeletions in the tuberous sclerosis 2 gene on patients' DNA. The simplicity, reproducibility, and precision of this approach makes it a powerful tool for a variety of genomic studies.

Recent developments in whole genome sequencing projects have all emphasized the importance of refined physical mapping tools that bridge the gap between establishing genetic maps and sequence-ready clones (*1*). Conventional approaches such as sequenced tagged sites (STS), content ordering of large insert clones [YAC or bacterial artificial chromosomes (BAC)] (*2*), and restriction mapping of redundant sets of smaller clones (*3*), used for the building of physical maps, are tedious and time consuming. New techniques developed for the direct visualization of clones, such as optical mapping (*4*) or fiber–fluorescence in situ hybridization (FISH) approaches (*5*, *6*), have either attempted to speed up these physical mapping steps or resolve some ambiguities of restriction mapping. However, none of these can be used routinely or independently from other methods. Moreover, for the purpose of genetic disease screening and molecular diagnostics, there is a need for efficient techniques within the resolution range of a few kilobases (kb) to a few hundred kilobases, a challenge addressed neither by polymerase chain reaction (PCR)–based approaches (*7*) nor by cytogenetics techniques (*8*).

We describe an approach for physical mapping and molecular diagnostics directed to the aforementioned resolution range.